Photoemission spectroscopy study of the lanthanum lutetium oxide/silicon interface

A. Nichau, M. Schnee, J. Schubert, A. Besmehn, J. Rubio-Zuazo et al.

Citation: J. Chem. Phys. **138**, 154709 (2013); doi: 10.1063/1.4801324
View online: http://dx.doi.org/10.1063/1.4801324
View Table of Contents: http://jcp.aip.org/resource/1/JCPSA6/v138/i15
Published by the American Institute of Physics.

Photoemission spectroscopy study of the lanthanum lutetium oxide/silicon interface

A. Nichau,[1,2] M. Schnee,[1,2] J. Schubert,[1,2] A. Besmehn,[3] J. Rubio-Zuazo,[4] U. Breuer,[3] P. Bernardy,[1,2] B. Holländer,[1,2] A. Mücklich,[5] G. R. Castro,[4] J. von Borany,[5] D. Buca,[1,2] and S. Mantl[1,2]

[1]*Peter Grünberg Institute 9 (PGI9-IT), Forschungszentrum Jülich, 52425 Jülich, Germany*
[2]*JARA-Fundamentals of Future Information Technologies, 52425 Jülich, Germany*
[3]*Central Division for Chemical Analysis (ZCH), Forschungszentrum Jülich, 52425 Jülich, Germany*
[4]*Spanish CRG BM25 Beamline-SpLine, European Synchrotron Radiation Facility (ESRF), Rue Jules Horowitz BP 220, F-38043 Grenoble, Cedex 09, France*
[5]*Institute of Ion Beam Physics and Materials Research, Helmholtz-Zentrum' Dresden-Rossendorf e.V., 01314 Dresden, Germany*

(Received 7 December 2012; accepted 25 March 2013; published online 18 April 2013)

Rare earth oxides are promising candidates for future integration into nano-electronics. A key property of these oxides is their ability to form silicates in order to replace the interfacial layer in Si-based complementary metal-oxide field effect transistors. In this work a detailed study of lanthanum lutetium oxide based gate stacks is presented. Special attention is given to the silicate formation at temperatures typical for CMOS processing. The experimental analysis is based on hard x-ray photoemission spectroscopy complemented by standard laboratory experiments as Rutherford backscattering spectrometry and high-resolution transmission electron microscopy. Homogenously distributed La silicate and Lu silicate at the Si interface are proven to form already during gate oxide deposition. During the thermal treatment Si atoms diffuse through the oxide layer towards the TiN metal gate. This mechanism is identified to be promoted via Lu–O bonds, whereby the diffusion of La was found to be less important. © *2013 AIP Publishing LLC*. [http://dx.doi.org/10.1063/1.4801324]

I. INTRODUCTION

Lanthanum lutetium oxide ($LaLuO_3$) has been shown to be a promising higher k dielectric.[1] Its high relative permittivity in the amorphous state of ∼32 in conjunction with low gate leakage current densities demonstrated in long channel MOSFETs may recommend its integration into future CMOS technology nodes.[1] For the sub-20 nm nodes an equivalent oxide thickness (EOT) below 0.7 nm is required. The tendency of rare earth oxides to form silicates could allow a high-k oxide in direct contact with Si neglecting the need of a low-k SiO_2 interlayer.[2] The successful integration of 3 nm $LaLuO_3$ in a MOSFET with a so-called "gate-first process," which requires high temperature annealing[3,4] for source/drain activation, resulted in a rather large EOT = 1.9 nm. However, integration of 6 nm $LaLuO_3$ employing a low thermal budget process of 400 °C[5] and 650 °C[6–8]) led to EOT = 16 and EOT = 1.4 nm extracted at flatband voltage $V_{fb} - 1$ V, respectively. Theoretically, an EOT of 1.0 nm and 1.4 nm is estimated from the reported permittivity. These results clearly indicate that during thermal processing an interface reaction happens at the high-k oxide/silicon channel interface. Moreover, cross-section transmission electron microscopy studies indicated slight diffusion of Ti into $LaLuO_3$ for 650 °C/10 min or 1000 °C spike anneal.[3,7] Therefore, the optimization of the $LaLuO_3$ integration requires a detailed knowledge of the thermal stability and the silicate formation within the gate stack.

The interfaces of interest in these studies are buried by a few tens of nanometers with high-k oxide and metal gate. In consequence, the interface chemistry of $Si/SiO_{2-x}/LaLuO_3$ and $LaLuO_3$/TiN before and after thermal processing is inaccessible to non-destructive laboratory XPS methods due to the reduced photoelectron escape depth and the low x-ray flux. Several methods were experimentally employed to investigate such buried interfaces.[9–11] Hard x-ray photoemission spectroscopy (HAXPES), which combines the concepts of laboratory photoemission spectroscopy with high energetic and high brilliance of synchrotron radiation, has been proven adequate and efficient in probing the chemical state of buried interfaces.[12,13] Furthermore, HAXPES extends the energy range and a measurement of orbitals with higher binding energy, e.g., Si 1*s* becomes possible. The measurement of Si 1*s* is important in combination with La since La 4*d* and Si 2*p* can overlap to a certain extend. Additionally, the Si 1*s* spectra are free of spin-orbit coupling in contrast to the coupling found in Si 2*p*.

In this contribution a detailed investigation of thermal treatments of $TiN_x/LaLuO_3$ gate stacks is presented with the respect to the device processing requirements. The stoichiometry and the chemical state of the interface elements are analyzed by HAXPES. A change of interface stoichiometry has then been correlated to electrical measurements obtained from similar processed MOS capacitors.

II. EXPERIMENTAL

The analyzed gate stack consists of 10 nm $LaLuO_3$ dielectric layers deposited by molecular beam deposition (MBD) at 450 °C[14] and 16 nm TiN_x metal layers deposited by physical vapor deposition (PVD). Prior to deposition, the Si (100) substrates were RCA cleaned[15] which forms a thin silicon chemical oxide (~1 nm). The metal layer stoichiometry was determined by Rutherford backscattering spectrometry in channeling direction (RBS/C) to reduce the Si background signal.[16] RBS was performed with 1.4 MeV He^+ at an incident angle of 0° and a scattering angle of −170°. The stoichiometry was Ti:N ≈ 1:0.95 for uncapped layers.

To study the interface reactions in the gate stack, the samples were annealed in a rapid thermal processing (RTP) system under N_2 ambient in the temperature range 400–1000 °C (post-deposition anneal (PDA)). For electrical characterization MOS capacitors were fabricated. The MOS capacitor samples were taken from the same wafer and annealed at 1000 °C for 5 or 60 s. Using a 200 nm Al hard mask the TiN is removed by reactive ion etching stopping on the high-k layer. Forming gas annealing (FGA) in 90% N_2/10% H_2 at a temperature of 450 °C for 10 min was carried out after MOS capacitor fabrication.

The HAXPES experiments were performed at the Spanish CRG (SpLine) beamline at the European Synchrotron Radiation Facility (ESRF) Grenoble. The kinetic energy of the incoming photons was 10, 12, and 14 keV at pass energy of 100 eV. The spectra, measured by a high voltage cylindrical sector analyzer Focus CSA 300/15,[17] were calibrated with respect to the position of the N 1*s* signal in TiN (binding energy BE = 397.0 eV[18]). The incident angle (beam respect to sample surface) was 5°, the emission angle (analyzer angle respect to sample normal) was 15°, and hence, beam respect to analyzer was 85° + 15° = 100° as in Ref. 13. The calibration of the energy scale was confirmed by the signal position of the Si 1*s* orbital from the Si substrate at 1839.2 eV.[18] The Gaussian peak width is calculated as explained in Ref. 17. The energy width of the beam line optics corresponds to 1.5 eV, 1.8 eV, and 2.1 eV for 10, 12, and 14 keV, respectively, and the analyzer intrinsic energy resolution is 1.5 eV. Hence, a total Gaussian width of 2.1, 2.3, and 2.6 eV was employed for 10, 12, and 14 keV, respectively. The energy resolution is hereby limited by the optics. It is independent of the kinetic energy due to the analyzer running in a fixed pass energy mode. For peak fitting a convolution of Lorentzian and Gaussian peak contributions was used. The Gaussian width was held fixed and the Lorentzian peak width was chosen constant where lifetime broadening was known from Ref. 19. The spectra were normalized with respect to photon flux, the photoionization cross sections, and detector transmission.[12] After HAXPES analysis, the unstructured stacks were analyzed by RBS and high-resolution transmission electron microscopy (HRTEM).

III. RESULTS AND DISCUSSIONS

A. HAXPES results

An advantage of the HAXPES method is the excitation of large cross section orbitals, like Si 1*s*, to screen the chemical state of a buried interface. This allows an efficient information access.

1. Si 1s orbital analyses

The silicon Si 1*s* spectra of the as-deposited and annealed sample obtained by HAXPES at 14 keV are presented in Fig. 1. All spectra were normalized to the as-deposited sample intensity of $Si^{\pm 0}$ which was present in every spectra (large EAL) and was subsequently subtracted from the annealed sample spectra. The plot shows the $Si^{\pm 0}$ intensity of the as-deposited sample *together* with the subtracted intensities of the annealed samples. The 600 °C annealed sample measurement was found identical to the as-deposited case. Specifically, this means that the resulting plots emphasize the change with respect to further thermal treatment. The large intensity for $Si^{\pm 0}$ indicates an information depth (ID) much larger compared to the information which comes from the thin interfacial layer (RCA clean substrate, $t_{SiO_2} = 1$ nm). The ID is the specimen thickness from which a specified percentage of the detected signal originates.[12] Often the ID is defined as three times the effective attenuation length (EAL). This corresponds to the depth from where approximately 95% of the signal originates.[20] The EAL is estimated from the TPP-2M formula[21] to amount to 19.5 nm at 14 keV.

The reaction between Si and $LaLuO_3$ and the final reaction products are strongly dependent on the annealing duration and temperature. For PDA between 400 °C and 600 °C and up to 60 s no additional silicate indication could be detected within the measurement resolution. The nomenclature for the formation of silicates was chosen as in Ref. 2.

First at 800 °C for 60 s Si-rich silicate bonds could be observed in the Si 1*s* orbital spectra,[2] whereby the major contribution can be identified as La-rich silicate (dashed line at 1841.5 eV). Finally, a 60 s PDA at 1000 °C leads to the

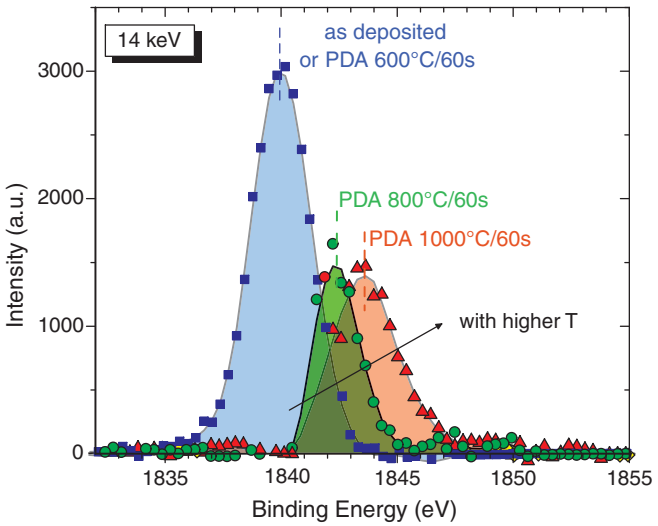

FIG. 1. HAXPES Si 1*s* spectra of the as-deposited and different annealed samples for photon energy of 14 keV. All spectra were normalized to the as-deposited sample intensity of $Si^{\pm 0}$ and its contribution was then subtracted from the annealed sample spectra. No difference could be obtained between PDA 600 °C/60 s and the as-deposited sample. At 800 °C the first interface change into silicate is visible.

formation of an Si-rich compound, seen at 1844 eV, most likely Si- and O-rich compounds, e.g., $La_2Si_2O_7$, and a La-rich silicate like La_2SiO_5 (1839 eV < BE < 1844 eV), less pronounced than at lower temperatures.

The integrated Si intensity of the annealed samples (spectrum of elemental Si and oxidation states) becomes larger compared to the signal of the as-deposited sample. Due to the constant ID in the sample Si is concluded to diffuse into the above-lying high-k layer.

2. La $3p_{3/2}$ orbital analyses

In Fig. 2 the HAXPES spectra of the La $3p_{3/2}$ orbitals, taken at 14 keV, before and after annealing are plotted. The sampling depth in terms of EAL was measured in Ref. 22 to amount to (14.7 ± 1.2) nm.

Directly after deposition, several binding states are identified in the La $3p_{3/2}$ orbitals by peak deconvolution: La–O at ~1126.0 eV, a La exchange satellite (La–O sat) at ~1129.0 eV and La silicate (La–O–Si) at 1132.6 eV. In addition, plasmons features are observed at +12.5 eV from the main peaks. The chemical shift indicates the reaction with a reactant of higher electronegativity (EN), like Si and Lu (Pauling $EN_{Si} = 1.9$, $EN_{Lu} = 1.27$, $EN_{La} = 1.1$) demonstrating the silicate formation at the high-k/Si interface.

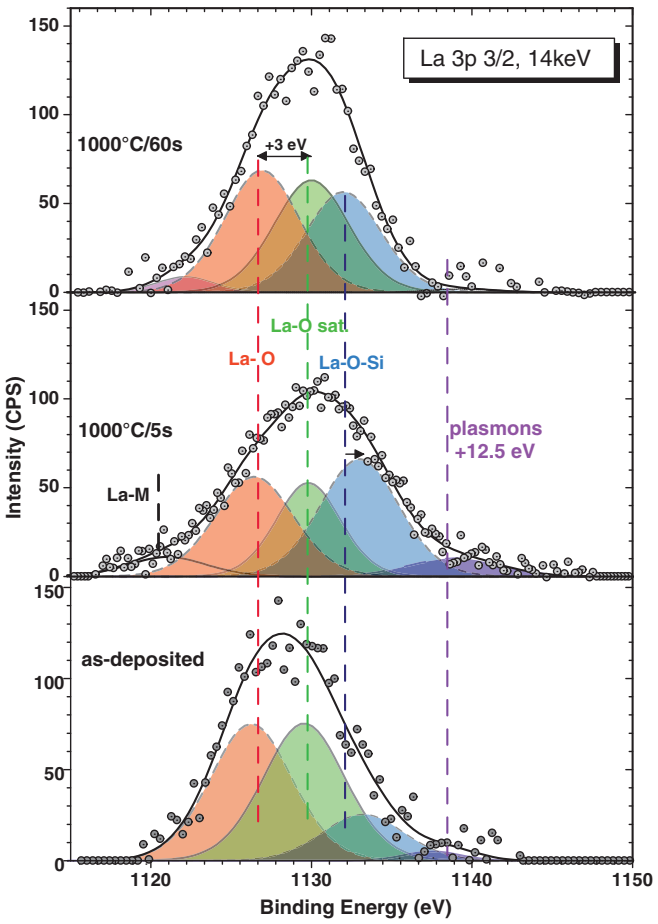

FIG. 2. HAXPES La $3p_{3/2}$ spectra of the as-deposited and annealed samples for photon energy of 14 keV. The following contributions are identified: La–O at 1126.3 eV, La–O–Lu at 1129.3 eV, and La–O–Si at 1132.5 eV plus plasmon features at +12.5 eV from the main peaks. The as-deposited sample shows ~−1.4 eV lower BE for La–O and La–O–Lu bindings.

A further partition in several silicate contributions as seen in Si 1*s* cannot be assessed here due to the aforementioned Gaussian peak width. The La silicate signal is therefore assumed as a single contribution. Accordingly, the BE is constraint within 3 eV(1841–1844 eV) to account for different amounts of bridging and non-bridging oxides,[2] BO and NBO, respectively. The upper limit was chosen with the reference value for SiO_2.[18] A change in BE marks then a change in the amount of NBO to BO. Lower BE is interpreted as La-rich(er) silicate and higher BE as oxygen and Si-rich(er) SiO_2-like bonds. Please note also that due to the higher Gaussian FWHM for hard x-ray optics, the peaks in our measurement added up to one broad convolution. Moreover, the spectra for $LaLuO_3$ are more difficult to deconvolute than for pure lanthanide, Ln_2O_3, because of the slight stoichiometric variations within the layer with different EN for La and Lu.

According to Teterin *et al.*[23,24] and Crecelius *et al.*[25] the occurrence of the satellite La–O–*Ln* in the La orbital spectra can be ascribed to many-body perturbation, i.e., shake-up processes. Missing charge transfer over the NBO in La–O–Si explains the absence of a satellite in the La–O–Si bonds. The measured satellite position ($\Delta E_{sat} \approx 3$eV) is within the expectations of Teterin's study for lower BE orbitals.

After annealing, the peak intensities change clearly and the peak convolution broadens. The observed contribution at BE ~1121.3 eV, whose intensity is less than 10% of the total La signal, indicates the occurrence of either additional shake-down processes, as described by Teterin *et al.* for La $4p$[23] or metallic La-bonds. The significance of this peak has to be investigated by complementary measurements and is highly depending on background subtraction. The peak deconvolution revealed La–O and La–O–Lu bonds with a +0.8 eV higher BE compared to the as-deposited samples. This energy shift is correlated with a reduced amount of La–O bonds per atom in favor of increasing atomic bond density to Si (La–O–Si). Thereby the electron bonds are closer correlated to La, resulting in higher BE for the replacement of La–O–La by La–O–Si bonds.

The silicate peak at 1132.8 eV for the 1000 °C/5 s anneal is found within 0.2 eV at the same position as in the non-annealed sample (1132.6 eV). This peak contribution increased after annealing in parallel to a reduction of La–O bonds. After a longer anneal (1000 °C/60 s), the silicate component is lowered in BE to 1132.0 eV, which may be explained by a larger amount of La-rich silicate in respect to SiO_2-like bonds.

3. Lu $3d_{5/2}$ orbital analyses

Lu–O and Lu–O–Si are present already after deposition. Silicate formation at the interface Si/$LaLuO_3$ is proved by this additional peak component at higher BE. The boundary silicate formation from Si orbital signals was also observed in prior annealing studies.[14] Here, the Lu $3d_{5/2}$ orbital (Fig. 3) of the as-deposited samples consists of a main contribution from

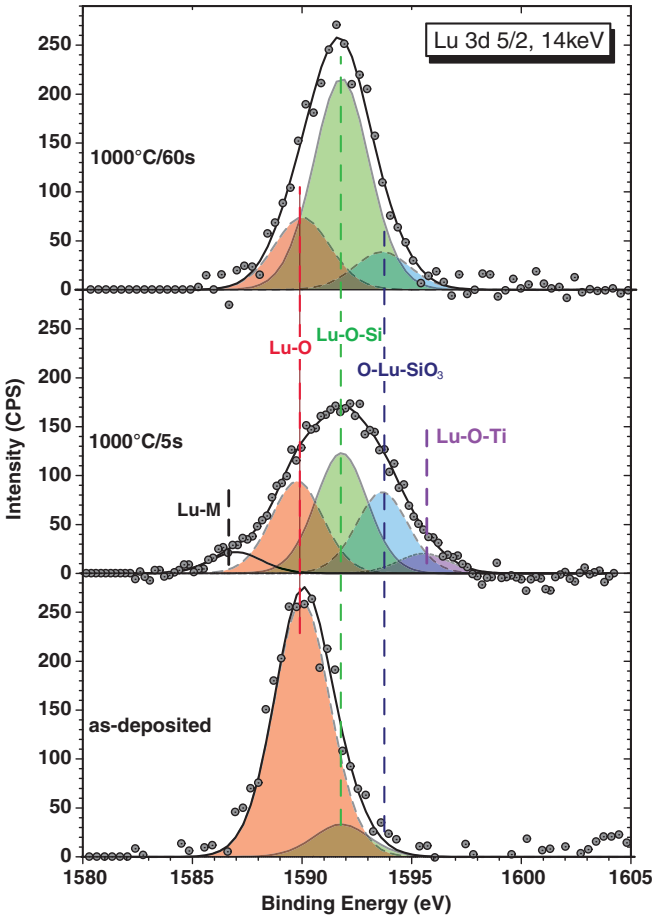

FIG. 3. HAXPES Lu $3d_{5/2}$ spectra of the as-deposited and annealed samples for photon energy of 14 keV. The following bonds are identified: Lu=O at 1589.9 eV, Lu–O–Si at 1591.8 eV. After annealing additional binding states occur. One is attributed to orthosilicate Lu–O–SiO_3 at 1593.8 eV.[31] After 5 s anneal a component at 1595.3 eV is present, which we attribute to more Lu–O–Ti bonds. Within the scan range of 1580–1600 eV no clear plasmon features were detected.

Lu–O at 1589.9 eV (±0.5 eV) and a minor silicate contribution (11%) at 1591.9 eV.

After annealing a variety of additional peaks are detected: For the 1000 °C anneal for 5 s a clear trend to form more Lu silicates and orthosilicates is present (Fig. 3, dotted lines): the component at 1591.8 and the one at 1593.8 eV are identified as silicate and orthosilicate complexes, respectively. The orthosilicates refer to a silicate containing the group SiO_4 in which the ratio of silicon to oxygen is 1–4, e.g., $Lu_{10}(SiO_4)_6O_3$. Interestingly, these peak contributions are positioned at rather high BE (Fig. 3). The oxygen rich complex shifts the BE to even higher values compared to normal bridging oxygen in Si-rich Ln–O–Si. These (Si-rich) *Ln*-orthosilicates complexes are claimed by other authors to form high quality silicate interfaces between *Ln* oxide and silicon layer as compared to *Ln*-rich silicates.[26] Si-rich silicates are believed to feature higher effective mobility in MOSFETs. Despite, in La no orthosilicates were detected, possibly due to the broad (Lorentzian) lifetime for the La 3*p* hampering the deconvolution for hard x rays.

A minor peak contribution (6% of the integrated signal) at 1595.3 eV is only present for the 5 s anneal. The additional component is interpreted with Lu–O–Ti bonds due to the argument of different electronegativity, which vanish again for the full silicate formation after 60 s anneal.

However, the peak position of the orthosilicates phase can also be identified via *Ln*–O–Ti bonds based on their electronegativity. A separation of Si or Ti to O bonds is difficult because of reduced energy resolution at high energy. Only for the 1000 °C/5 s sample a minor contribution at 1586.7 eV for intermetallic bonds (Lu–M) is indicated.

After 1000 °C anneal for 60 s the Lu–O component decreases compared to the as-deposited sample. Thereby, the orthosilicate compound at 1593.8 eV decreases in density and is replaced by a strong silicate contribution, seen at 1591.8 eV. The difference to the 5 s anneal is significant: The Lu–O contribution is screened already at 10 keV (not shown here) and increases only slightly with ID. Despite this little contribution left from the oxide, a large amount of Lu compound is transformed into a silicate. The ID in the material stack remains the same for fixed photon energy (see Fig. 3). Therefore, this transformation is equivalent with an up-diffusion of Si into the *Ln*-oxide. For Lu $3d_{5/2}$ no significant plasmon features was found within 40 eV scan range.

In former studies the amorphous structure in $LaLuO_3$ was shown to be maintained during high temperature anneals.[27] The silicate formation is an important second parameter to control in gate stack engineering. However, based on the higher relative permittivity of the silicates compared to SiO_2, it has been shown that the control of the silicate formation can lead to low EOT and high capacitances.[2,26,28,29]

4. HAXPES qualitative depth analyses

A non-destructive but qualitative depth profile analyses can be obtained by varying the incoming x-ray energy and applying the orbital deconvolution approach (Fig. 4). The integrated peak areas are compared on a relative scale. The energy shift observed for La silicate was summarized as a single silicate formation to increase readability). Remarkably, the

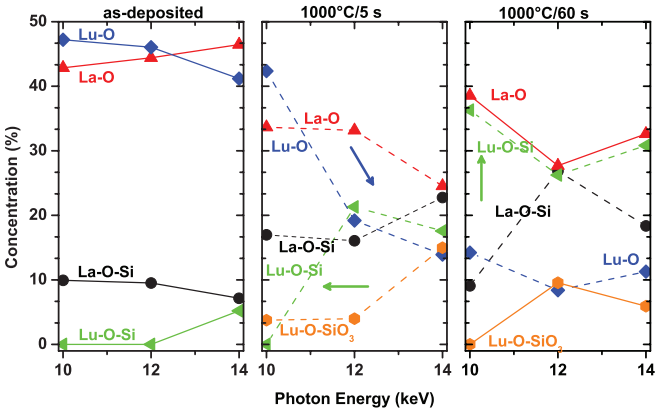

FIG. 4. HAXPES depth profile vs. photon energy using the integrated peak areas obtained by deconvolution of the orbitals. For the as-deposited sample La silicate is found through the layer and Lu silicate only at the interface. The amount of La silicate increases during annealing. More pronounced is the up-diffusion and reaction of silicon to form Lu silicate. Based on this quantitative analysis the diffusion of Si seems to be mainly promoted by the generation of Lu–O–Si bonds and less by La bonds.

as-deposited sample contains already La silicate while Lu silicate is only present at the interface to Si (i.e., detected only at 14 keV photons energy). For the 5 s annealed sample, the La silicate amount increases but remains homogeneously distributed. More important, Lu silicate contribution increases rapidly from the substrate into the gate oxide layer on the cost of a reduced amount of Lu–O bonds.

Comparing the 5 and 60 s annealing the orthosilicates seen for Lu decreased again (cf. also Fig. 3). A maximum of only 13% Lu–O bonds density remains after longer temperature treatment. Both Lu and La silicate compounds density increases along with a reduction of La–O bonds. However, at the upper interface ($LaLuO_3$/TiN) a higher La oxide signal compared to La silicate is obtained: the La silicate accumulates in the gate oxide layer in contrast to Lu silicate which accumulates at the top and bottom interfaces.

To conclude, the reduction of Lu oxide to Lu silicate is the driving force behind the up-diffusion of silicon. This effect is less pronounced for La and, for long annealing, the relative amount of La oxide increases again at the top and the bottom interfaces.

5. Metal gate analyses and Ti diffusion study

The reactions taking place in the top TiN layer have been investigated by HAXPES via the orbitals N 1*s* (not shown here) and Ti 1*s*. The normalized total intensities are shown in Fig. 5 for photon energy of 14 keV. The total intensity of Ti 1*s* after annealing equals, within the measurement errors, the intensity before annealing. For the samples undertaking a 1000 °C for 5 s annealing an *ex situ* 2 nm Si-capping was deposited prior annealing to prevent additional TiO_x formation on the surface. However, this *ex situ* treatment does not prevent the prior oxidation of TiN. Further experiments but with *in situ* deposited Si-capping of TiN need to be taken into account. The comparison of the spectra in Fig. 5 shows that no further oxidation during annealing takes place, for the present stoichiometry of TiN. A percentage ratio of 64–32 for TiN to TiO_x compounds was extracted for the uncapped, as-deposited sample. Since this large amount of TiO_x is already present prior annealing, no reduction of $LaLuO_3$ or interfacial SiO_2 (scavenging effect) is seen and is even thermodynamically unfavorable for La reduction by Ti.

A minor Ti–O–*Ln* bond density is present at 4975.5 eV for 14 keV. This binding state increases slightly with temperature from 6% in the as-deposited case to 7% for 1000 °C for 60 s annealing but not significant to prove a diffusion of TiN into $LaLuO_3$ layer. Here the observed Ln–O–Ti peak in Ti 1*s* differs in magnitude from observations in La and Lu. Since the information depth and effective attenuation length for Lu3*d*, La3*p*, and Ti 1*s* differ, the bonds at the upper interface may be more significant in the Ti 1*s* peak. For the 1000 °C/5 s sample the background signal was measured up to 5115 eV to incorporate the role of the plasmon features on peak deconvolution. Two huge plasmon features at 4982 eV and 4995 eV at a FWHM = 11.6 eV were detected. The incorporation of the additional information leads to similar peak fits besides a minor shift of the Ti–O–Ln peak from 4975.5 eV

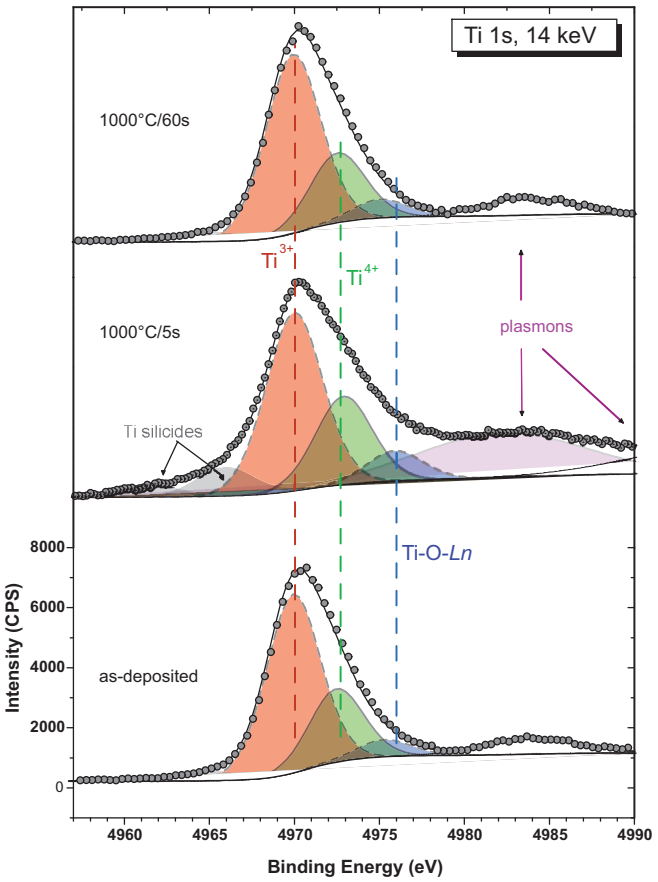

FIG. 5. HAXPES Ti 1*s* spectra of the as-deposited and annealed samples at photon energy of 14 keV). The as-deposited sample shows contributions from Ti^{3+} (TiN) and Ti^{4+} (TiO_x). The long time between sample preparation and beam line experiment has led to oxidation of the TiN layer (Shirley background subtraction, ratio 64:32% for TiN:TiO_x). A minor contribution at higher BE than Ti^{4+} could be identified due to the peaks asymmetry.

(as deposited) to 4975.9 eV. This deviation remains acceptable on the basis of the wider definition of the background function and the peak width (FHWM ~5.3 eV). Thus future experiments can be limited to a scan range within the plasmon decay.

Comparing the Ti 1*s* spectra at 10 keV (Fig. 6) the overall intensity decreases by 9% for the 60 s annealed sample, originating from an intensity decrease of the original Ti^{3+} peak of TiN. Therefore, a slight diffusion of Ti deeper into the oxide layer under reduction of TiN can be attested. The slight shift to higher BE present is attributed to more Ti=O binding states after annealing. It is worth to note that, neither at 10 keV nor at 14 keV did additional peak asymmetry arise from a clear interaction of Ti with La or Lu. Likewise, more oxygen is bond to Ti but few bindings to *Ln* are present. A limitation for the further quantification is the use of a Shirley background for Ti(N). The Shirley background subtraction is still under debate for Ti[30] but used in the absence of better solutions.

B. RBS analyses

RBS measurements obtained from equally processed samples are presented in Fig. 7. After annealing at

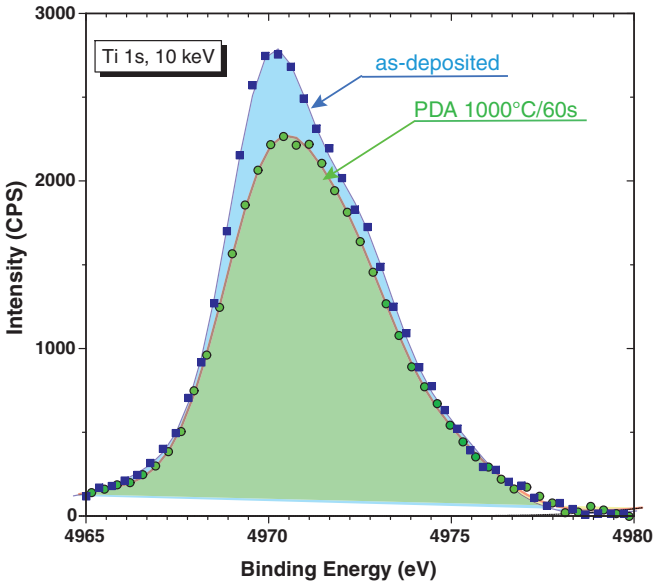

FIG. 6. HAXPES Ti 1*s* spectra (background subtracted) after 1000 °C/60 s anneal and as-deposited for photon energy of 10 keV. The lower information depth at 10 keV compared with 14 keV leads to lower intensities after annealing meaning Ti diffusion into the gate stack.

1000 °C/60 s broadening in the signals from La and Lu supports the thickness increase of the oxide layer. Moreover, the signal intensity decrease is explained by a change of the stoichiometry by adding Si in the oxide layer. A change in the silicon signal due to silicate formation could not be proved by either simulation or measurement due to overlapping with the strong Si substrate signal. This limitation is due to the scattering of He^+ ions deep in the substrate. For the 1000 °C/5 s anneal and lower temperature processes the stoichiometry of the stack determined by RBS stays almost constant, i.e., the effects seen in HAXPES cannot be further quantified by RBS. The initial stoichiometry was determined to be La:Lu:O = 1:1:2.9.

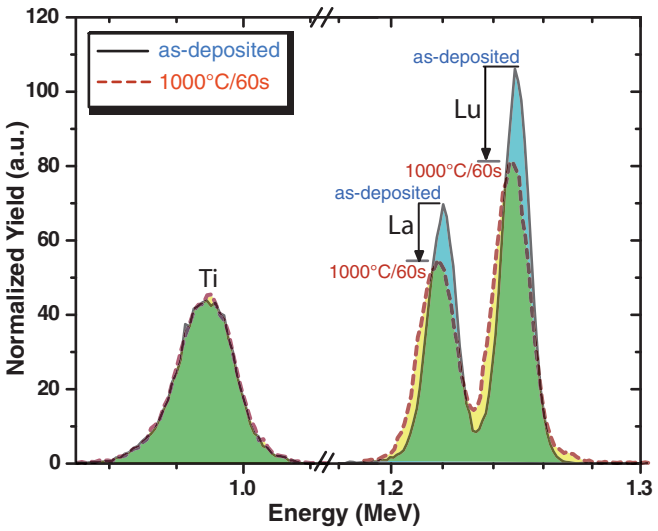

FIG. 7. RBS measurements of the annealed samples compared to as-deposited. The signals of La and Lu decrease and broaden after annealing, which corresponds to a relative decrease of the *Ln* concentration in the oxide layer.

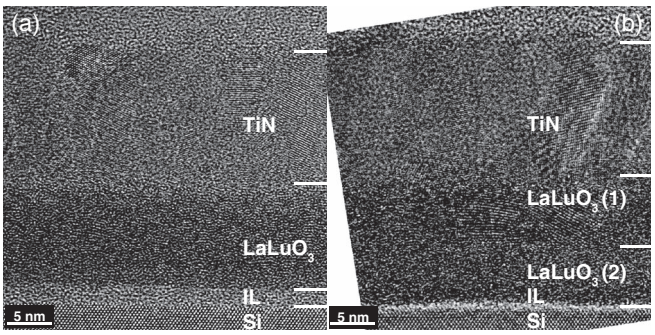

FIG. 8. HRTEM of the as-deposited (a) and 1000 °C for 5 s annealed sample. The thickness of TiN is about 16 nm. The $LaLuO_3$ layer thickness is ~10.4 nm in (a) and 13.3 nm in (b). The separation of $LaLuO_3$ into two layers could be due to the aforementioned silicate formation.

C. HRTEM analysis

HRTEM analyses were performed employing an image-corrected FEI Titan 80-300 microscope to assess detailed information on the material morphology and layer thickness increase, seen in the physical and chemical analysis. In Fig. 8 the as-deposited sample is shown in comparison to the sample annealed at 1000 °C for 5 s. The thickness of as-deposited $LaLuO_3$ (11 nm) is in reasonable agreement with the RBS data. The TiN thickness is determined to be ~16 nm. Lattice planes visible in the top layer confirm the polycrystalline structure of TiN in contrast to the amorphous $LaLuO_3$. After annealing (1000 °C / 5 s) a clear thickness increase from 11 nm to 14 nm (~+27%) is measured. The thickness increase is also in agreement with reports for La silicate (+20%) by Kakushima *et al.*[2] In parallel the thick interfacial layer transformed to a single silicate layer. This transformation can be explained by the HAXPES results (Fig. 1). After deposition the film consists of a Si-rich interfacial layer and $LaLuO_3$. After annealing, the Si-rich phase transformed into a La-rich silicate consuming partly the high-k oxide. An additionally seen separation of $LaLuO_3$ into two equal sized layers can also be aligned with the photoemission data by the determined silicate formation in $LaLuO_3$. The equally separated layers seen by material contrast are due to the different densities of $LaLuO_3$ and its silicates below. The nano-crystalline features seen for the $LaLuO_3$ layer might be attributed to ~9% Ti diffusion into the layer seen by HAXPES. A clear contrast between high-k oxide and TiN is still observed, thus the slight diffusion of Ti does not lead to significant density changes. However, further studies need to be done on this aspect.

D. Electrical characterization of MOS capacitors

The capacitance-voltage characteristics (C-V) for 10 nm thick $LaLuO_3$ layers are shown in Fig. 9. The capacitance equivalent thickness (CET) was extracted at gate voltage $V_g = V_{fb} + 1.5V$, whereby V_{fb} means the flatband voltage of the MOS gate stack. After 450 °C FGA, a CET = 3.1 nm is extracted as expected for an oxide κ-value of ~30 and 1 nm interfacial oxide. The knowledge of interface chemistry and the gate oxide layer thickness is important for the determination of the relative permittivity.

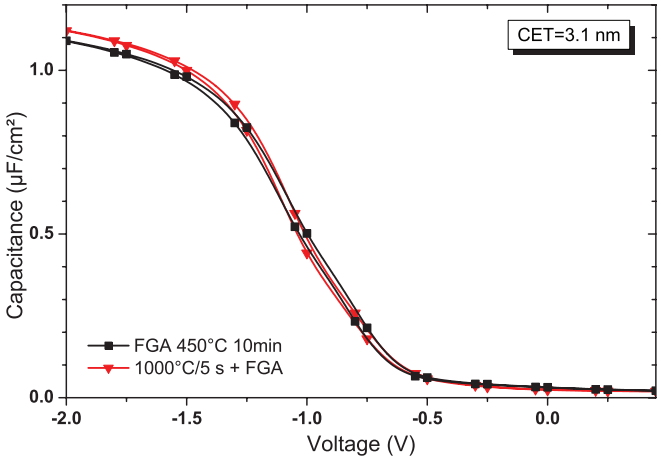

FIG. 9. C-V characteristics for different sample annealing. The CET was extracted at V_{fb} + 1.5V. Comparable CET values are found before and after annealing.

For a typical source/drain activation temperature of Si MOSFETs of 1000 °C for 5 s similar CET and V_{fb} are found without *in situ* Si-capping of TiN. For experiments with TiN/HfO_2 gate stacks a change in the flatband voltage of −0.3 eV is found in contrast to the constant value in conjunction with $LaLuO_3$. The constant flatband voltage is explained by the *ex situ* capping of TiN blocking nitrogen out-diffusion. For a sample annealed at 1000 °C/60 s V_{fb} shifted to more negative voltage under reduced capacitance and is currently under investigation.

IV. CONCLUSIONS

A detailed spectroscopy study of thermal processed Si/$LaLuO_3$/TiN gate stacks was presented. Hard x-ray XPS, RBS, and HRTEM were used to analyze the chemical changes and explain the transition from oxides to silicate phases. The major advantage offered by HAXPES is the possibility to separate the silicate growth and the atomic diffusion. A clear difference between silicate formation coordinated to La and Lu was found.

TiN might not be the best candidate as metal gate on $LaLuO_3$ since TiN was found to intermix with the underlying oxide layer in small fractions (9%).

La and Lu silicates are already present after deposition and seem to be grown during MBD (fraction maximum 10%). During annealing La silicate is constantly formed. Lu diffuses significantly into the oxide layer and the majority of the initial Lu-bonds are transformed into Lu silicate. For shorter annealing Lu orthosilicate formation was found which could be beneficial for the effective mobility in MOSFETs. Our quantitative analysis proves that the diffusion of Si is mainly promoted via the generation of Lu–O–Si bonds and less by La bonds. Thereby, the high-κ oxide is consumed, which displays a tradeoff between interfacial silicate formation (higher κ than SiO_2) and intact high-κ material. Based on our experiments, engineering of the interfacial layer between high-κ oxide and Si is most promising for La-based oxides, whereby Lu tends to rather fast silicate formation.

ACKNOWLEDGMENTS

This work was partially supported by the project KZWEI which is funded in line with the technology funding for regional development (ERDF) of the European Union and by funds of the Free State of Saxony. We would like to thank the SpLine staff for their valuable help in carrying out this research. Neal Fairley of CasaXPS Ltd. is acknowledged for providing all XPS import filters and his continued expert support. We thank Martin M. Frank of IBM Research for valuable discussions of the orthosilicate phases.

[1]J. M. J. Lopes, E. Durgun Özben, M. Roeckerath, U. Littmark, R. Luptak, S. Lenk, M. Luysberg, A. Besmehn, U. Breuer, J. Schubert, and S. Mantl, Microelectron. Eng. **86**, 1646 (2009).
[2]K. Kakushima, T. Koyanagi, K. Tachi, J. Song, P. Ahmet, K. Tsutsui, N. Sugii, T. Hattori, and H. Iwai, Solid-State Electron. **54**, 720 (2010).
[3]A. Nichau, E. Durgun Özben, M. Schnee, J. M. J. Lopes, A. Besmehn, M. Luysberg, L. Knoll, S. Habicht, V. Mussmann, R. Luptak, S. Lenk, J. Rubio-Zuazo, G. R. Castro, D. Buca, Q.-T. Zhao, J. Schubert, and S. Mantl, Solid-State Electron. **71**, 19 (2012).
[4]A. Nichau, E. Durgun Özben, M. Schnee, J. M. J. Lopes, A. Besmehn, M. Luysberg *et al.*, "Lanthanum Lutetium oxide integration in a gate-first process on SOI MOSFETs," in *Conference Proceedings, Ulis 2011 Ultimate Integration on Silicon* (IEEE, 2011), pp. 1–4.
[5]E. Durgun Özben, J. M. J. Lopes, A. Nichau, M. Schnee, S. Lenk, A. Besmehn, K. K. Bourdelle, Q.-T. Zhao, J. Schubert, and S. Mantl, IEEE Electron Device Lett. **32**, 15 (2011).
[6]W. Yu, B. Zhang, Q.-T. Zhao, J.-M. Hartmann, D. Buca, A. Nichau, R. Luptak, J. M. J. Lopes, S. Lenk, M. Luysberg, K. K. Bourdelle, X. Wang, and S. Mantl, Solid-State Electron. **62**, 185 (2011).
[7]W. Yu, E. Durgun Özben, B. Zhang, A. Nichau, J. M. J. Lopes, R. Luptak, S. Lenk, J.-M. Hartmann, D. Buca, K. K. Bourdelle, J. Schubert, Q.-T. Zhao, and S. Mantl, in *2010 10th IEEE International Conference on Solid-State and Integrated Circuit Technology* (IEEE, 2010), pp. 875–878.
[8]W. Yu, B. Zhang, Q.-T. Zhao, J.-M. Hartmann, D. Buca, A. Nichau, E. Durgun Özben, J. M. J. Lopes, J. Schubert, B. Ghyselen, and S. Mantl, in *Proceedings of 6th Workshop of the Thematic Network on Silicon-on-Insulator Technology (EUROSOI)* (IEEE, 2010), pp. 25–26.
[9]J. Rubio-Zuazo, E. Martinez, P. Batude, L. Clavelier, F. Soria, A. Chabli, G. R. Castro, D. G. Seiler, A. C. Diebold, R. McDonald, C. M. Garner, D. Herr, R. P. Khosla, and E. M. Secula, AIP Conf. Proc. **931**, 329–333 (2007).
[10]C. Gaumer, E. Martinez, S. Lhostis, F. Fillot, P. Gergaud, B. Detlefs, J. Roy, Y. Mi, J.-P. Barnes, J. Zegenhagen, A. Chabli, E. M. Secula, D. G. Seiler, R. P. Khosla, D. Herr, C. Michael Garner, R. McDonald, and A. C. Diebold, AIP Conf. Proc. **1173**, 40–44 (2009).
[11]T. Hantschel, C. Demeulemeester, A. Suderie, T. Lacave, T. Conard, and W. Vandervorst, MRS Proc. **1184**, 226 (2009).
[12]J. Rubio-Zuazo and G. R. Castro, Surf. Interface Anal. **40**, 1438 (2008).
[13]J. Rubio-Zuazo, P. Ferrer, and G. R. Castro, J. Electron Spectrosc. Relat. Phenom. **180**, 27 (2010).
[14]J. M. Lopes, E. Durgun Özben, M. Schnee, R. Luptak, A. Nichau, A. Tiedemann, W. Yu, Q.-T. Zhao, A. Besmehn, U. Breuer, M. Luysberg, S. Lenk, J. Schubert, and S. Mantl, ECS Trans. **35**, 461 (2011).
[15]W. Kern, J. Electrochem. Soc. **137**, 1887 (1990).
[16]B. J. Burrow, J. Vac. Sci. Technol. A **4**, 2463 (1986).
[17]J. Rubio-Zuazo, M. Escher, M. Merkel, and G. R. Castro, Rev. Sci. Instrum. **81**, 043304 (2010).
[18]NIST X-ray Photoelectron Spectroscopy Database, Version 4.0, National Institute of Standards and Technology, Gaithersburg, 2008.
[19]M. O. Krause and J. H. Oliver, J. Phys. Chem. Ref. Data **8**, 329 (1979).
[20]ISO, ISO 18115: Surface Chemical Analysis—Vocabulary, 2001.
[21]S. Tanuma, C. J. Powell, and D. R. Penn, Surf. Interface Anal. **17**, 927 (1991).
[22]A. Nichau, J. Rubio-Zuazo, M. Schnee, G. R. Castro, J. Schubert, and S. Mantl, Appl. Phys. Lett. **102**, 031607 (2013).

[23]Y. A. Teterin and A. Y. Teterin, Russ. Chem. Rev. **71**, 347 (2002).
[24]Y. A. Teterin, A. Y. Teterin, A. M. Lebedev, and K. E. Ivanov, J. Electron Spectrosc. Relat. Phenom. **137–140**, 607 (2004).
[25]G. Crecelius, G. K. Wertheim, and D. N. E. Buchanan, Phys. Rev. B **18**, 6519 (1978).
[26]K. Kakushima, K. Okamoto, and K. Tachi, in *Technical Digest of IWDTF 2008: International Workshop on Dielectric Thin Films for Future ULSI Devices: Science and Technology* (JJAP, 2008), pp. 9–10.
[27]M. Roeckerath, T. Heeg, J. M. J. Lopes, J. Schubert, S. Mantl, A. Besmehn, P. Myllymäki, and L. Niinistö, Thin Solid Films **517**, 201 (2008).
[28]T. Kawanago, K. Tachi, J. Song, K. Kakushima, P. Ahmet, K. Tsutsui, N. Sugii, T. Hattori, and H. Iwai, Microelectron. Eng. **84**, 2235 (2007).
[29]K. Kakushima, K. Okamoto, T. Koyanagi, K. Tachi, M. Kouda, T. Kawanago, J. Song, P. Ahmet, K. Tsutsui, N. Sugii, T. Hattori, and H. Iwai, in *2009 Proceedings of the European Solid State Device Research Conference* (IEEE, 2009), pp. 403–406.
[30]M. Oku, K. Wagatsuma, and S. Kohiki, Phys. Chem. Chem. Phys. **1**, 5327 (1999).
[31]A. Navrotsky, American Mineralogist **79**, 589 (1994); online at http://ammin.geoscienceworld.org/content/79/7-8/589.short.